minerals

Article

Distribution of Glycerol Dialkyl Glycerol Tetraethers (GDGTs) in Carbonate-type and Sulfate-type Lacustrine Sediments: Insight into the Influence of Ionic Composition on GDGTs

Yongxin Chen [1], Xilong Zhang [1], Wen Qi [2], Gaoqing Zhang [3], Yu Pei [1,4], Xuan Fang [1], Yanqing Xia [1,]* and Shengyin Zhang [1,]*

[1] Northwest Institute of Eco-Environment and Resources, Chinese Academy of Sciences/Key Laboratory of Petroleum Resources, Lanzhou 730000, China
[2] Research Institute of Petroleum Exploration and Development - Northwest (NWGI), PetroChina, Lanzhou 730020, China
[3] College of Vanadium and Titanium, Panzhihua University, Panzhihua 617000, China
[4] University of Chinese Academy of Sciences, Beijing 100049, China
* Correspondence: yqxia@lzb.ac.cn (Y.X.); zhangshengyin@nieer.ac.cn (S.Z.)

Keywords: carbonate-type saline lake; sulfate-type saline lake; ionic composition; GDGTs; reconstructed temperature

Citation: Chen, Y.; Zhang, X.; Qi, W.; Zhang, G.; Pei, Y.; Fang, X.; Xia, Y.; Zhang, S. Distribution of glycerol dialkyl glycerol tetraethers (GDGTs) in carbonate-type and sulfate-type lacustrine sediments: Insight into the influence of ionic composition on GDGTs. *Minerals* **2022**, *12*, 1233. https://doi.org/10.3390/min12101233

Academic Editor(s): Qi Fu and Thomas Gentzis

Received: 14 August 2022
Accepted: 24 September 2022
Published: date

1. Major elemental chemistry analysis

Major elemental chemistry of the samples was determined by Inductively Coupled Plasma Mass Spectrometer (ICP-MS; 7850 Agilent). Approximately 100m g of each sample was acid digested in Digestion tank with a mixture of 1mL HF and 0.5mL HNO_3 at 185℃ for 24 h. After cooling, the tank was heat to dry. Then the sample was added 5 ml nitric acid and heated at 130℃ for 3h. Finally, the sample was volutized to 50 ml for ICP-MS analysis.

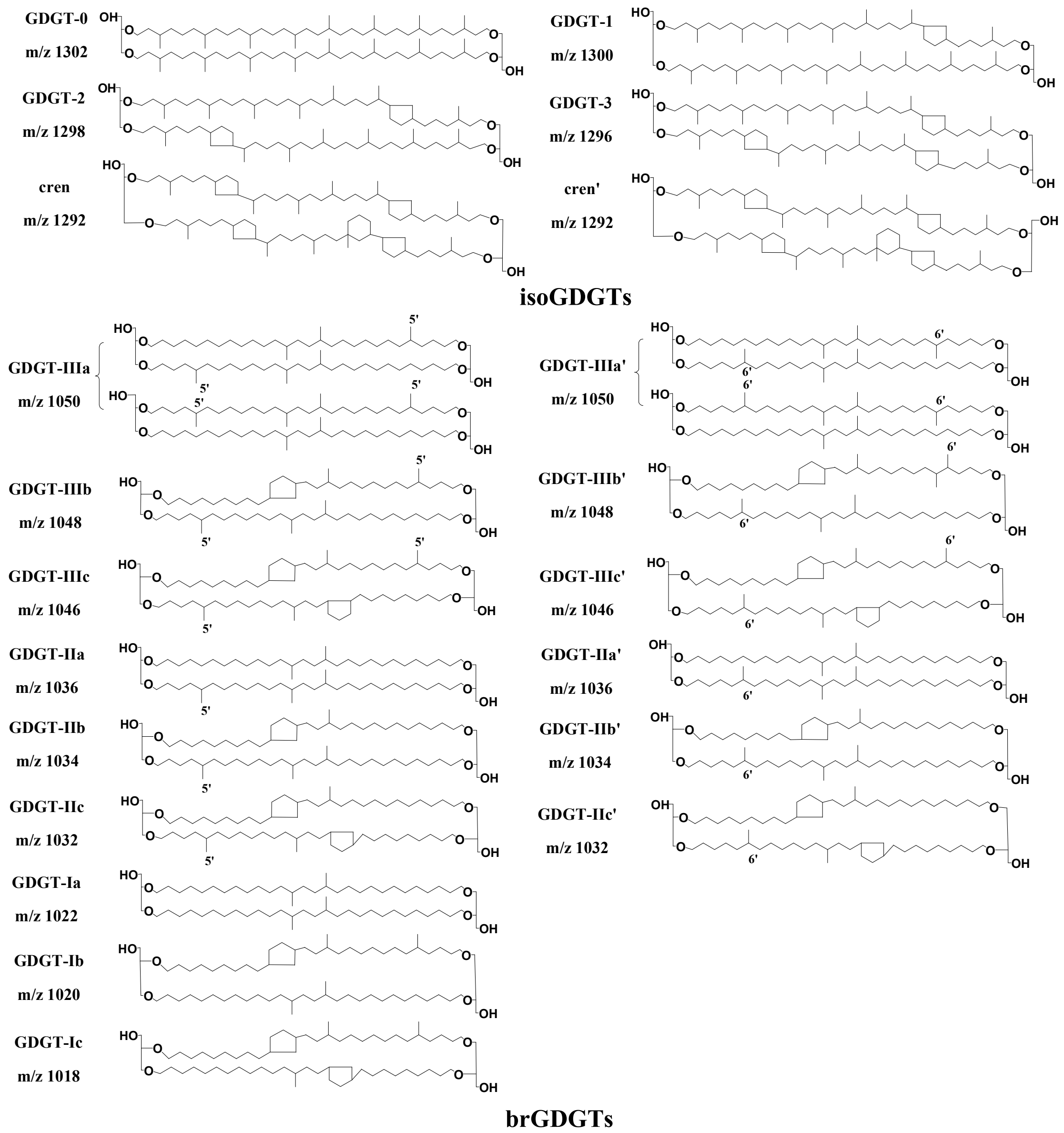

Figure S1. Structures and molecular ion mass/charge ratios (m/z) for glycerol dialkyl glycerol tetraethers (GDGTs).

Table S1. Different calculation formulas for GDGTs.

No.	Formulas[a]	References
1	TEX_{86} = (GDGT-2 + GDGT-3 + Cren') / (GDGT-1 + GDGT-2 + GDGT-3 + Cren')	[1]
2	BIT = (Ia + IIa + IIa' + IIIa + IIIa') / (Ia + IIa + IIa' + IIIa + IIIa' + cren)	[2]
3	ACE = archaeol / (archaeol + GDGT-0) × 100	[3]
4	$R_{i/b}$ =∑isoGDGTs / ∑brGDGTs	[4]
5	MBT = (Ia + Ib + Ic) / (Ia + Ib + Ic + IIa + IIa' + IIb + IIb' + IIc + IIc' + IIIa + IIIa' + IIIb + IIIb' + IIIc + IIIc')	[5]
6	MBT' = (Ia + Ib + Ic) / (Ia + Ib + Ic + IIa + IIa' + IIb + IIb' + IIc + IIc' + IIIa + IIIa')	[6]
7	CBT = −log[(Ib + IIb + IIb') / (Ia + IIa + IIa')]	[5]
8	MBT'_{5ME} = (Ia + Ib + Ic) / (Ia + Ib + Ic + IIa + IIb + IIc + IIIa)	[7]
9	CBT_{5ME} = −log[(Ib + IIb) / (Ia + IIa)]	[7]
10	MBT'_{6ME} = (Ia + Ib + Ic) / (Ia + Ib + Ic + IIa' + IIb' + IIc' + IIIa')	[7]
11	CBT_{6ME} = −log[(Ib + IIb') / (Ia + IIa')]	[7]
12	IR_{6Me} = (IIa' + IIb' + IIc' + IIIa' + IIIb' + IIIc') / (IIa + IIa' + IIb + IIb' + IIc + IIc' + IIIa + IIIa' + IIIb + IIIb' + IIIc + IIIc')	[7]
13	$[x]_{5ME}$ = x / IIIa + IIIb + IIIc + IIa + IIb + IIc + Ia + Ib + Ic) $[y]_{6ME}$ = y / IIIa' + IIIb' + IIIc' + IIa' + IIb' + IIc' + Ia + Ib + Ic)	[8]
14	$MAAT_{Tierney2010}$ = 11.8 + 32.5 × MBT − 9.3 × CBT	[9]
15	$MAAT_{Tierney2010'}$ = 50.47 − 74.18 × f(IIIa+IIIa') − 31.60 × f(IIa+IIa') − 34.69 × f(Ia)	[9]
16	$MAAT_{Loomis}$ = 2.54 − 5.02 × CBT + 45.28 × MBT	[10]
17	$MAAT_{Loomis2012'}$ = 36.9 − 50.1 × f(IIIa+IIIa') − 35.5 × f(IIa+IIa') − 1.0 × f(Ia)	[10]
18	$MAAT_{Sun2011}$ = 6.803 − 7.062 ×CBT + 37.090 × MBT	[11]
19	$MSAT_{Pearson2011}$ = 20.9 + 98.1 × f(Ib) − 12.0 × f(IIa+IIa') − 20.5 × f(IIIa+IIIa')	[12]
20	$MSAT_{Foster2016}$ = 18.7 + 80.3 × f(Ib) − 25.3 × f(IIa+IIa') − 19.4 × f(IIIa+IIIa') + 369.9 × f(IIIb)	[13]
21	$MAAT_{Gunther2014}$= −3.84 + 9.84 × CBT + 5.92 × MBT'	[14]
22	Growth $T_{Dang2018}$ = −29.73 × $[IIIa]_{5ME}$ + 91.97 × $[IIIb]_{5ME}$ − 551.02 × $[IIIc]_{5ME}$ + 22.65 × $[IIb]_{5ME}$ + 3.19 × $[Ib]_{5ME}$ − 4.23 × $[IIIa']_{6ME}$ − 147.28 × $[IIIb']_{6ME}$ + 460.10 × $[IIIc']_{6ME}$ − 14.59 × $[IIa']_{6ME}$ + 40.02 × $[IIb']_{6ME}$ − 230.78 × $[IIc']_{6ME}$ + 7.54 × $[Ia]_{6ME}$ + 29.48 × $[Ic]_{6ME}$ + 12.73	[8]

Table S2. Fractional abundances of individual isoGDGTs and the concentrations of total isoGDGTs for the 13 surface sediments.

Sample	Fractional abundance of isoGDGTs						Total isoGDGTs
	GDGT-0	GDGT-1	GDGT-2	GDGT-3	cren	cren'	(ug/g TOC)
HH	0.884	0.027	0.018	0.007	0.058	0.006	12.63
DL	0.840	0.031	0.032	0.009	0.079	0.008	43.08
NL	0.866	0.061	0.054	0.010	0.009	0.001	319.78
HM	0.931	0.019	0.037	0.003	0.009	0.001	20.93
SU	0.903	0.038	0.014	0.004	0.037	0.004	165.76
HD	0.897	0.020	0.067	0.003	0.011	0.002	191.07
DK	0.923	0.022	0.015	0.004	0.032	0.004	47.10
WH	0.672	0.032	0.037	0.013	0.229	0.016	3.02
GC	0.890	0.038	0.027	0.003	0.037	0.005	55.61
LN	0.756	0.076	0.123	0.022	0.020	0.003	33.95
BL	0.765	0.078	0.040	0.007	0.103	0.008	3.45
LH	0.848	0.021	0.030	0.007	0.086	0.009	3.54
HY	0.814	0.061	0.046	0.006	0.064	0.009	14.97

Table S3. Fractional abundances of individual brGDGTs and the concentrations of total brGDGTs and GDGTs for the 13 surface sediments. 1

Sample	Fractional abundance of brGDGTs															brGDGTs (ug/g TOC)	Total GDGTs (ug/g TOC)
	IIIa	IIIa'	IIIb	IIIb'	IIIc	IIIc'	IIa	IIa'	IIb	IIb'	IIc	IIc'	Ia	Ib	Ic		
HH	0.019	0.187	0.000	0.000	0.000	0.000	0.037	0.293	0.011	0.081	0.003	0.012	0.274	0.062	0.021	12.01	24.64
DL	0.105	0.098	0.000	0.000	0.000	0.000	0.182	0.148	0.041	0.107	0.005	0.014	0.162	0.116	0.021	119.07	162.15
NL	0.046	0.138	0.007	0.004	0.001	0.000	0.171	0.148	0.036	0.048	0.003	0.005	0.305	0.073	0.015	206.46	526.24
HM	0.043	0.106	0.000	0.000	0.000	0.000	0.172	0.137	0.029	0.048	0.006	0.007	0.375	0.059	0.018	3.06	23.99
SU	0.030	0.176	0.002	0.002	0.000	0.000	0.141	0.219	0.028	0.023	0.003	0.008	0.322	0.037	0.010	199.80	365.56
HD	0.039	0.184	0.000	0.000	0.000	0.000	0.104	0.192	0.022	0.100	0.003	0.010	0.258	0.073	0.014	14.93	206.00
DK	0.043	0.182	0.000	0.000	0.000	0.000	0.082	0.185	0.015	0.079	0.003	0.009	0.332	0.056	0.013	19.89	66.99
WH	0.039	0.227	0.000	0.000	0.000	0.000	0.046	0.265	0.039	0.101	0.003	0.007	0.163	0.095	0.014	1.18	4.20
GC	0.025	0.206	0.000	0.000	0.000	0.000	0.034	0.358	0.018	0.087	0.027	0.007	0.175	0.046	0.016	5.34	60.94
LN	0.023	0.134	0.000	0.000	0.000	0.000	0.031	0.264	0.022	0.122	0.050	0.005	0.249	0.092	0.008	1.73	35.67
BL	0.034	0.263	0.000	0.000	0.000	0.000	0.051	0.267	0.050	0.058	0.007	0.006	0.173	0.067	0.025	2.92	6.38
LH	0.032	0.209	0.000	0.000	0.000	0.000	0.019	0.269	0.024	0.050	0.003	0.005	0.351	0.028	0.010	1.46	5.01
HY	0.021	0.150	0.000	0.000	0.000	0.000	0.060	0.301	0.019	0.066	0.003	0.003	0.294	0.076	0.008	4.76	19.73

2

Table S4. The concentrations of major element for the 13 surface sediments.

Sample	Concentrations (mg/L)										
	Al	**Ba**	**Ca**	**Fe**	**K**	**Mg**	**Na**	**Mn**	**P**	**Si**	**Sr**
HH	59.72	1.26	18.34	13.51	46.55	4.75	60.00	0.14	0.25	0.52	0.32
DL	116.29	1.40	125.76	39.56	47.00	20.62	44.74	0.72	0.61	1.12	1.38
NL	113.82	1.20	143.29	25.82	36.79	26.69	49.85	0.76	0.67	0.97	1.29
HM	92.94	0.67	301.81	48.32	29.12	33.76	20.74	1.01	0.87	0.81	1.63
SU	107.86	1.10	76.51	25.31	41.46	116.85	44.98	0.45	0.52	1.03	3.03
HD	67.99	1.19	25.57	15.28	46.44	9.30	91.85	0.17	0.34	0.66	0.44
DK	112.92	1.08	87.52	36.50	42.49	68.01	82.09	0.69	0.61	1.60	1.27
WH	111.16	0.90	113.31	58.08	39.53	33.20	83.10	1.04	0.93	0.87	1.07
GC	44.13	0.16	126.33	25.18	16.35	47.08	178.05	0.36	0.59	0.83	2.56
LN	89.24	0.72	60.38	35.61	33.98	41.24	83.15	0.53	0.52	0.84	0.46
BL	73.03	0.47	169.25	36.49	25.17	47.36	92.16	0.67	0.75	1.22	4.12
LH	64.01	0.50	127.65	38.61	29.19	48.24	136.99	0.66	0.66	0.78	1.83
HY	87.36	0.61	131.88	44.51	30.79	44.41	64.74	0.80	0.68	0.98	1.64

References

1. Schouten, S., Hopmans, E.C., Schefuß, E., Sinninghe Damsté, J.S. Distributional variations in marine crenarchaeotal membrane lipids: a new tool for reconstructing ancient sea water temperatures? Earth Planet. Sci. Lett. 2002, 204, 265-274, https://doi.org/10.1016/S0012-821X(02)00979-2.
2. Hopmans, E.C.; Weijers, J.W.; Schefuß, E.; Herfort, L.; Damsté, J.S.S.; Schouten, S. A novel proxy for terrestrial organic matter in sediments based on branched and isoprenoid tetraether lipids. *Earth Planet. Sci. Lett.* **2004**, *224*, 107–116, https://doi.org/10.1016/j.epsl.2004.05.012.
3. Turich, C.; Freeman, K.H. Archaeal lipids record paleosalinity in hypersaline systems. *Org. Geochem.* **2011**, https://doi.org/10.1016/j.orggeochem.2011.06.002.
4. Xie, S.; Pancost, R.; Chen, L.; Evershed, R.P.; Yang, H.; Zhang, K.; Huang, J.; Xu, Y. Microbial lipid records of highly alkaline deposits and enhanced aridity associated with significant uplift of the Tibetan Plateau in the Late Miocene. *Geology* **2012**, *40*, 291–294, https://doi.org/10.1130/g32570.1.
5. Weijers, J.W.; Schouten, S.; Donker, J.C.V.D.; Hopmans, E.C.; Damsté, J.S.S. Environmental controls on bacterial tetraether membrane lipid distribution in soils. *Geochim. et Cosmochim. Acta* **2007**, *71*, 703–713, https://doi.org/10.1016/j.gca.2006.10.003.
6. Peterse, F.; van der Meer, J.; Schouten, S.; Weijers, J.W.; Fierer, N.; Jackson, R.B.; Kim, J.-H.; Sinninghe Damsté, J.S. Revised cali-bration of the MBT-CBT paleotemperature proxy based on branched tetraether membrane lipids in surface soils. Geochim. Cosmochim. Acta 2012, 96, 215–229, https://doi.org/10.1016/j.gca.2012.08.011.
7. De Jonge, C.; Stadnitskaia, A.; Fedotov, A.; Damsté, J.S.S. Impact of riverine suspended particulate matter on the branched glycerol dialkyl glycerol tetraether composition of lakes: The outflow of the Selenga River in Lake Baikal (Russia). *Org. Geochem.* **2015**, *83-84*, 241–252, https://doi.org/10.1016/j.orggeochem.2015.04.004.
8. Dang, X.; Ding, W.; Yang, H.; Pancost, R.D.; Naafs, B.D.A.; Xue, J.; Lin, X.; Lu, J.; Xie, S. Different temperature dependence of the bacterial brGDGT isomers in 35 Chinese lake sediments compared to that in soils. *Org. Geochem.* **2018**, *119*, 72–79, https://doi.org/10.1016/j.orggeochem.2018.02.008.
9. Tierney, J.; Russell, J.; Eggermont, H.; Hopmans, E.; Verschuren, D.; Damsté, J.S. Environmental controls on branched tetraether lipid distributions in tropical East African lake sediments. *Geochim. et Cosmochim. Acta* **2010**, *74*, 4902–4918, https://doi.org/10.1016/j.gca.2010.06.002.
10. Loomis, S.E.; Russell, J.M.; Ladd, B.; Street-Perrott, F.A.; Damsté, J.S.S. Calibration and application of the branched GDGT temperature proxy on East African lake sediments. *Earth Planet. Sci. Lett.* **2012**, *357-358*, 277–288, https://doi.org/10.1016/j.epsl.2012.09.031.
11. Sun, Q., Chu, G., Liu, M., Xie, M., Li, S., Ling, Y., Wang, X., Shi, L., Jia, G., Lü, H. Distributions and temperature dependence of branched glycerol dialkyl glycerol tetraethers in recent lacustrine sediments from China and Nepal. J. Geophy. Res.-Biogeosci. 2011, 116, 2005-2012, https://doi.org/10.1029/2010JG001365.
12. Pearson, E.J., Juggins, S., Talbot, H.M., Weckström, J., Rosén, P., Ryves, D.B., Roberts, S.J., Schmidt, R. A lacustrine GDGT-temperature calibration from the Scandinavian Arctic to Antarctic: renewed potential for the application of GDGT-paleothermometry in lakes. Geochimi. Cosmochimi. Ac. 2011, 75, 6225- 6238, https://doi.org/10.1016/j.gca.2011.07.042.
13. Foster, L.C.; Pearson, E.J.; Juggins, S.; Hodgson, D.A.; Saunders, K.M.; Verleyen, E.; Roberts, S.J. Development of a regional glycerol dialkyl glycerol tetraether (GDGT)–temperature calibration for Antarctic and sub-Antarctic lakes. *Earth Planet. Sci. Lett.* **2016**, *433*, 370–379, https://doi.org/10.1016/j.epsl.2015.11.018.
14. Günther, F.; Thiele, A.; Gleixner, G.; Xu, B.; Yao, T.; Schouten, S. Distribution of bacterial and archaeal ether lipids in soils and surface sediments of Tibetan lakes: Implications for GDGT-based proxies in saline high mountain lakes. *Org. Geochem.* **2014**, *67*, 19–30, https://doi.org/10.1016/j.orggeochem.2013.11.014.